Design of Electromagnetic Drive Module for Micro-gyroscope

Nan-Chyuan Tsai*, Jiun-Sheng Liou, Chih-Che Lin, Tuan Li

Abstract—For micro-gyroscopes, the angular rate detection components have to oscillate forwards and backwards alternatively. An innovative design of micro-electromagnetic drive module is proposed to make a Π-type disc reciprocally and efficiently rotate within a certain of angular interval. Twelve Electromagnetic poles enclosing the thin disc are designed to provide the magnetic drive power. Isotropic etching technique is employed to fabricate the high-aspect-ratio trench, so that the contact angle of wire against trench can be increased and the potential defect of cavities and pores within the wire can be prevented. On the other hand, a Π-type thin disc is designed to conduct the pitch motion as an angular excitation, in addition to spinning, is exerted on the gyroscope.

The efficacy of the micro-magnetic drive module is verified by the commercial software, *Ansoft Maxewll*. In comparison with the conventional planar windings in micro-scale systems, the magnetic drive force is increased by 150%.

Keywords—Micro-gyroscope, Micro-Electromagnetic, Micro Actuator

I. INTRODUCTION

Micro-actuators have been the popular research objectives for two decades. However, most of them are constrained to be designed for pretty particular purposes. For example, the micro-fluid pump is mostly used for the micro-fluidic channels on bio-chips [1]. The thermally activated cantilever beam is often employed for switch functions [2]. The electrostatic combs are normally used for linear motion [3-4]. The piezoelectric actuators are usually used for low-power transfer [5]. In comparison, the applications of electrical motors in macro-scale systems are fairly diversified and considerably wide-ranged. If micro-motors in micro-scale fields can be well developed and become mature, then the actuation mechanism will get more commercialized and convenient to promote the applications of micro-devices.

One early proto-type of micro-motors was reported by Fan in 1988 [6]. The thickness of the disc (instead of spindle in macro-scale motors) is about $1.0 \sim 1.5 \mu m$ and the rotation speed in $500 RPM$ as the applied voltage is $350V$. The induced maximum torque is of several pico-Newton-meters. Nowadays, the types of micro-motors, according to drive patterns, can be categorized as "*Electrostatic*" and "*Electromagnetic*". Though the micro-machining for the electrostatic type is relatively simpler, the induced torque and rotation speed of disc are both low. As to the electromagnetic type, the induced torque can reach the order of several nano-Newton-meters, the fabrication is relatively complicated and expensive. The bottle neck of the fabrication technique is how to make 3-D (spiral) windings. LIGA (Lithographie GalVanoformung Abformung) can be employed to make high aspect ratio but is expensive and not suitable for mass production from the viewpoint of cost. Therefore, planar winding (i.e., 2-D windings) is often utilized [7]. However, the drive power generated by planar windings is fairly limited and sometimes insufficient. Ahn ever reported the 3-D windings by electroplating technique [8], including toroidal-meander type and solenoid-bar type. However, the required high-aspect-ratio trench cannot be completely filled up by the electroplated copper since a few cavities within the wire are generated during the electroplating process. By utilizing the isotropic property of HNA (HF/HNO$_3$/CH$_3$COOH) etchant, the contact angle of wire against the trench can be increased so that the coherence between electroplated copper and the trench can be much improved. By employing the commercial softwares, *IntelliSuite* and *Ansoft Maxewll*, the feasibility of isotropic etch, incorporated with electroplating process, and the efficacy of induced magnetic flux field are both verified respectively.

Unlike micro-motors, the proposed micro-electromagnetic drive module is to make the seismic disc reciprocally rotate, within a certain of angular interval, clockwise and counter-clockwise about the principal axis (i.e., Z-axis). The reciprocally rotating disc plays the role of angular rate detection component in micro-gyroscopes so that it has to tilt about Y-axis (X-axis) if an angular excitation is exerted on the gyroscopes about X-axis (Y-axis). Therefore, a Π-type thin disc is proposed, including a central bearing and a set of bushing, to conduct the pitch motion, in addition to the spinning about Z-axis.

In order to drive the disc to rotate, twelve EM (Electromagnetic) poles are designed and allocated to enclose the disc. All the EM poles are with iron cores at the center and wound by spiral electroplated wires, i.e., they are of solenoid type.

II. DESIGN OF ELECTROMAGNETIC DRIVE MODULE

A. Design of Π-type Disc

Since the disc is spinning about the principal axis (i.e., Z-axis), it always needs a bearing set to ensure the offset of the geometric center of the disc is limited below a certain of level.

However, concurrently the disc has to respond by tilting about Y-axis (or X-axis) if an external angular rate about X-axis (or Y-axis) is exerted as long as the rotating disc plays the role of detection component for a gyroscope. That is, the gap between disc and bearing has to be narrowed down so that the spinning axis of disc is not offset much. However, the resolution of angular rate measure is accordingly reduced since the tilt angle is limited by the mechanical stop due to the collision between disc and bearing, as shown in Fig. 1(a). In order not to sacrifice the resolution of angular rate measure and preserve the limited gap, an innovative design of disc, named as Π-type disc hereafter, is proposed and shown in Fig. 1(b). Its section view is shown in Fig. 1(c).

B. Allocation of Four 3-phase EM Poles

The innovative design of micro-electromagnetic drive module is proposed to make a Π-type thin disc reciprocally and efficiently rotate within a certain of angular interval about Z-axis. Twelve EM poles, with iron cores at the center and wound by electroplated copper wires, enclosing the thin disc are designed to provide the magnetic drive power, shown in Fig. 2. Each triplet of the EM poles is composed of *Pole A*, *Pole B* and *Pole C*, which are supplied with 3-phase AC current. Totally there are 4 triplets. The Π-type thin disc can be driven by the EM poles onto which the supplied 3-phase AC current is sequentially shifted. Concurrently, the tangential force and radial force to the disc are induced, shown in Fig. 3, by the sinusoidal magnetic field and eddy current respectively. Both of them will be derived and discussed in next section.

III. Drive for Reciprocal Rotation of Disc

A. Analysis of Induced Magnetic Force by EM Poles

The supplied 3-phase current to the Electromagnetic (EM) pole triplet, (A, B, C), can be expressed by:

$$i_A = I_m \sin(\omega t) \tag{1}$$

$$i_B = I_m \sin(\omega t - 2\pi/3) \tag{2}$$

$$i_C = I_m \sin(\omega t - 4\pi/3) \tag{3}$$

where I_m is the amplitude of the AC current and ω the angular frequency. By Ampere's Law, the induced magnetic flux density by *Pole A* can be described by:

$$\oint_C \vec{B} \cdot d\vec{\ell} = \mu_0 N i_A \tag{4}$$

where $\vec{B}$ is the magnetic flux density, $\vec{\ell}$ path of the magnetic flux, μ_0 the permeability in air, N the number of windings on *Pole A*, and i_A the supplied current to *Pole A*. The approximate magnetic flux path around *Pole A* is shown in Fig. 4. By assuming the iron-loss and fringing-effect can be neglected, the average of the induced magnetic flux density by *Pole A* can be approximated by:

$$\overline{B}_A = \mu_0 N i_A / \ell_t \tag{5}$$

where $\ell_t = s_0 + l_r + l_{ei}$ is the total length of the path for the

induced magnetic flux by *Pole A*, s_0 the equivalent path length with respect to the center of *Pole A*, l_r the air gap between *Pole A* and Disc, and l_{ei} the skin depth of eddy current at disc. The topologic diagram by setting the circular position along the 12 EM poles (i.e., 4 triplets totally) as the X-axis is shown in Fig. 5. Since B_A is a periodic function with respect to angular position, θ, it can be expressed by Fourier Series:

$$B_A = \sum_{n=1}^{\infty} \frac{4\mu_0 N i_A}{n\pi\ell_t} \sin(\frac{n\pi}{\tau} S_a) \cos(\frac{n\pi}{\tau} \cdot (\theta + \phi)) \tag{6}$$

where τ is the pitch between any two adjacent triplets, i.e., $\tau = R\pi/2$, as shown in Fig. 5, R the radius of disc, and $2S_a$ the width of windings, shown in Fig. 4. By solely taking the first term of (6), i.e., $n = 1$, the resulted magnetic flux density by the EM Triplet #1, $(A1, B1, C1)$, can be described below:

$$B = B_{A1} + B_{B1} + B_{C1} = \frac{B_0}{\ell_t} \cos(\omega t - 2(\theta + \phi)) \tag{7a}$$

$$B_0 = \frac{6\mu_0 N I_m}{\pi} \sin(S_a \pi / \tau) \tag{7b}$$

where B_0 is hereby named as the magnetic intensity factor which is a constant. From (7a), it is noted that the induced magnetic field is time-varying and a function of position of disc, i.e., θ and ϕ.

By Faraday's Law, two types of EMF (Electro Motive Force) are induced by the sinusoidal magnetic field, namely, one is Motional EMF, e_t, and the other Transformer EMF, e_r:

$$\oint_C \vec{E} \cdot \vec{d} = e_t + e_r \tag{8a}$$

$$e_t = \oint_C (\vec{u} \times \vec{B}) \cdot d\vec{l} \tag{8b}$$

$$e_r = -\int_S \frac{\partial \vec{B}}{\partial t} \cdot d\vec{s} \tag{8c}$$

where $|\vec{u}| = R(\dot{\theta} + \dot{\phi}) - v_S$ is the relative velocity of disc with respect to the induced magnetic field, v_S the synchronized speed, i.e., the speed of magnetic field alternation. Accordingly, two types of induced current are generated by e_t and e_r. The former type of current, i_t, is induced by the tangential interaction between disc and the magnetic field. The latter type of current, i_r, is the eddy current induced within the skin depth of the disc. By applying Len's Law, the Motional EMF, e_t, can be obtained:

$$e_t = \oint_c (\vec{u} \times \vec{B}) \cdot d\vec{l} = 2\int_0^D [(\vec{u}\hat{a}_\varphi) \times (\vec{B}\hat{a}_r)] \cdot dh\hat{a}_z$$

$$= \frac{2R(N_S - \dot{\theta})B_0 D}{\ell_t} \cos(\omega t - 2\theta - 2\phi) \tag{9}$$

where N_S is the synchronous angular velocity (RPM) of the sinusoidal magnetic field, and D the thickness of the disc. The associated current density and current, due to e_t, are described

as follows respectively:

$$J_t = \frac{i_t}{A} = \frac{8(N_S - \dot{\theta})B_0 D}{\pi l_{ei}(s_0 + l_r)\sqrt{R_t^2 + (\omega L_t)^2}} \cos(\omega t - 2\theta - 2\phi)$$

$$(10a)$$

$$i_t = e_t / \sqrt{R_t^2 + (\omega L_t)^2} \qquad (10b)$$

where A is the equivalent section area of the disc passing by the EM pole triplet. R_t and L_t are the resistance and inductance of the disc respectively. They can be evaluated as follows:

$$A = l_{ei} R \int_0^{\pi/4} d\theta = \pi R l_{ei} / 4 \qquad (11)$$

$$R_t = \frac{l}{\sigma A} = \frac{8D + 2\pi R}{\sigma \pi R l_{ei}} \qquad (12)$$

$$L_t = \frac{\mu_0 ND}{3(s_0 + d + l_{ei})} + \frac{\mu_0 \pi D}{6(s_0 + d + l_{ei})} = \frac{\mu_0 D(2N + \pi)}{6(s_0 + d + l_{ei})}$$

$$(13)$$

where σ is the conductance coefficient of aluminum (i.e., the material of disc), and d gap between disc and EM pole triplet. Since $\rho = 3.7 \times 10^7 \ (1/m \cdot \Omega)$ is relatively large so that the magnitude of reluctance, $\sqrt{R_t^2 + (\omega L_t)^2}$, can be reduced to ωL_t. Applying Lorentz's Law, the tangential force on disc by the EM pole triplet can be obtained:

$$\vec{F}_t = \vec{J}_t \times \vec{B} = \frac{8(N_S - \dot{\theta})B_0^2 D}{\pi l_{ei}(s_0 + l_r)^2 \omega L_t} \cos^2(\omega t - 2\theta - 2\phi)$$

$$= \Gamma_t \frac{(N_S - \dot{\phi} - \dot{\theta})I_m^2}{(s_0 + l_r)^2 \omega} \cos^2(\omega t - 2\theta - 2\phi)$$

$$(14)$$

where the attraction force coefficient in the tangential direction, Γ_t, is defined as follows:

$$\Gamma_t = \frac{288\mu_0^2 N^2 D \cdot \sin^2(S_a \pi / \tau)}{\pi^3 L_t l_{ei}} \qquad (15)$$

On the other hand, the repulsive magnetic force on the disc by the EM pole triplet in the radial direction can be obtained:

$$\vec{F}_r = \vec{J}_r \times \vec{B} = \frac{\omega B_0^2 RD}{\pi R l_{ei} \ell_t^2 \omega L_r} \sin(2\omega t - 4\theta - 4\phi) \, \hat{a}_r \qquad (16)$$

where the repulsive force coefficient in the radial direction, Γ_r, is defined as follows:

$$\Gamma_r = \frac{18\mu_0^2 N^2 RD \cdot \sin^2(S_a \pi / \tau)}{\pi^2 L_r} \qquad (17)$$

From the viewpoint of mechanics, (14) and (16) are the forces exerting on the disc to make it rotate (major motion mode) and translate (side-effect).

B. Simulation and Discussion for Magnetic Flux Distribution

By employing the commercial software package, *Ansoft Maxwell*, the induced magnetic flux distribution and flux density by the EM poles are investigated in this section. Assume the width of deposited wire, the spacing of any two adjacent wires, and the supplied current to the windings are $20\mu m$, $20\mu m$ and $100mA$ respectively. The magnetic flux distribution and density induced by the proposed U-type EM poles is shown in Fig. 6(a). In comparison to the planar EM poles, whose magnetic flux distribution is shown in Fig. 6(b), the flux density is enhanced by 150% (i.e., from $6.5mTesla$ to $2.5mTesla$).

In addition, the most significant feature of the micro-motor is the torque-speed curve, on which the appropriate radius of the disc can be determined. Though the sensitivity and resolution can be both enhanced if the rotation speed of disc is increased, i.e., the radius of disc is decreased, the corresponding torque will be accordingly reduced. They can be shown in Fig. 7 and Fig. 8 respectively. Based on the trade-off rule, the radius of the disc is designed as $2500\mu m$ in our work. The Torque/Speed curve is shown in Fig. 9, under various applied voltage to the EM poles. In our work $V_R = 10V$. $\omega_{max}^{V_R}$ denotes the maximum rotational speed of the disc under applied voltage equal to V_R. $\omega_{max}^{V_R} = 3000Hz$ as $V_R = 10V$ in this paper. Similarly, $T_{max}^{V_R}$ is the maximum torque of the disc under applied voltage equal to V_R. ω represents the disc speed. T is the torque of the disc. On the other hand, if the drive frequency is tuned, the torque output of the disc is accordingly altered, as shown in Fig. 10. It is also noted that the maximum torque occurs at the intermediate rotational speed of disc. This is similar to the conventional induction-type electric-motors. Based on Fig. 9 and Fig. 10, the optimal power output of the micro-motor can be obtained by the tuning policy of VVVF (Variable Voltage Variable Frequency).

IV. FABRICATION OF U-TYPE ELECTROMAGNETIC POLES

The purpose of the proposed design of the U-type Electromagnetic Poles is to account for the defects of conventional 3-D fabrication process on solenoid-type windings [8]. The innovative fabrication design takes advantage of isotropic etching technique to make the walls of trenches non-vertical and outwards so that the contact angle of wire against trench is increased. It is shown in Fig. 11.

The merits of the obtuse-angle trenches includes:

a). to prevent generation of void and cave during electroplating process,

b). to enhance the stability of windings by the increased contact angle, and

c). merely a single photo-mask is required for the photo-lithography process.

The complete windings can be further divided into two portions: U-type Solenoid and Capped Windings.

A. U-type Solenoid

The so called U-type solenoid is, in fact, the low-half windings, from the sideview, and the enclosed iron core. It is shown in Fig. 12(a). Before copper electroplated, the substrate has to be micro-machined at first so that the obtuse-angle

trenches are constructed, shown in Fig. 12(b). The finished product, including the capping windings, is shown in Fig. 12(c). The fabricated process of the U-type Solenoid is shown in Fig. 13. Details are as follows:

(a) First of all, the undesired fine particles, organic substance, metal ions and native oxide on the surface of the <1 0 0 >-oriented silicon wafer is cleaned by the RCA (Radio Corporation of America) standard procedure. A thin film of silicon nitride (Si_3N_x) is deposited on the wafer by PECVD (Plasma Enhanced Chemical Vapor Deposition). This layer of Si_3N_x is used as the Etching Mask prepared for the HNA ($HF/HNO_3/CH_3COOH$) isotropic etching which will be undertaken later.

(b) A layer of photo-resist AZ-4620, with thickness $7\mu m$, is deposited onto the thin film in (a) by automatic spin coating system and then photo exposure process is undertaken so that the etching mask made by Si_3N_x is patterned and defined.

(c) The wafer is etched by the isotropic etchant, i.e., HNA solution, so that the obtuse-angle trenches with depth $200\mu m$ can be constructed. The HNA isotropic etchant is composed by HF, HNO_3 and CH_3COOH solutions. It can etch different shape and depth of trenches by tuning the relative proportion ratio of solution compositions and the etching time. In this work, $HF:HNO_3:CH_3COOH = 27 : 43 : 30$ and etching time = 12 mins are employed. The SEM and OM images of Obtuse-angle Trenches after HNA Etching are shown in Fig. 14.

(d) By using ICP (Inductively Coupled Plasma), the etching mask of Si_3N_x is removed.

(e) A layer of aluminum ($A\ell$) is deposited on the wafer by E-beam evaporator. The thickness of $A\ell$ layer is $150nm$ and the material $A\ell$ is not etched by ICP so that this layer can be used as an etching mask for deep dry etching. Then photo exposure process is undertaken so that the etching mask made by $A\ell$ is patterned and defined.

(f) By using ICP, the housing for U-type solenoid is constructed.

(g) The etching mask in (f) is removed by $A\ell$ etchant.

(h) A new layer of photo-resist AZ-4620 is coated and patterned by photo-lithography so that the trajectory of coil windings can be well defined.

(i) A seed layer of chromium (Cr), with thickness 1000 Å, is deposited by E-beam evaporator at first to enhance the coherence efficacy of copper layer which is to be deposited in the follow-up electroplating process.

(j) The photo-resist is removed by *Lift-off* in the Acetone solution. The seed layer of chromium can be defined.

(k) The copper layer (i.e., the low-half windings) is deposited onto the seed layer (Cr) by electroplating. It is noted that the applied current and concentration of electroplating solution have to be well controlled so that the undesired bubbles would not be generated.

B. Capped Windings

The so called Capped Winding is shown in Fig. 12(a). They are to be connected with the low-half windings so that a complete inductance is finished. The details of the fabrication process are as follows:

(l) A layer of photo-resist AZ-4620 is coated by spin coater and then patterned by photo-lithography.

(m) A layer of polyimide is coated by spin coater and patterned by *Life-off*. The polyimide can be insulated between the copper windings and iron core which is to be fabricated later.

(n) A layer of photo-resist is coated and then patterned.

(o) A seed layer of chromium (Cr), with thickness 1000 Å, is deposited by E-beam evaporator.

(p) The iron core is deposited onto the seed layer (Cr) by electroplating.

(q) A layer of photo-resist is coated and then patterned.

(r) A layer of polyimide is coated by spin coater and patterned by *Life-off*.

(s) A layer of photo resist is coated and then patterned.

(t) By using E-beam Evaporator, a seed layer of chromium (Cr), with thickness 1000 Å, is deposited and patterned by photo-lithography.

(u) Finally, the copper layer of capping windings is deposited onto the seed layer (Cr) by electroplating.

V. CONCLUSIONS

An innovative design of EM (Electromagnetic) poles to drive a Π-type thin disc to reciprocally and efficiently rotate within a certain of angular interval about the principal axis is proposed and verified by computer simulations. The major contributions of this paper are:

a). to fabricate the 3-D spiral windings, enclosing iron cores at the center, by employing isotropic etching technique so that the contact angle of the wire against the trench for housing the electroplated copper is much increased.

b). to propose the design and fabrication procedures of the U-type EM poles.

c). to derive and verify the induced magnetic attractive force to drive the Π-type thin disc to rotate up to $3000Hz$.

In comparison with planar windings, the induced magnetic force by the U-type solenoid is increased by 150%. The proposed design of the U-type solenoid can prevent the defect of conventional 3-D windings, i.e., the cavities and pores within the copper wire due to the high-aspect-ratio trench which cannot be completely filled up by the electroplated copper.

The material of the Π-type thin disc has to be limited to the ones that can efficiently experience the induced magnetic force by variable reluctance. The side effect by the Eddy current along the circular edge of the disc, which leads to a certain level of position offset of the disc, can be overcome by a feedback control loop which is usually necessary even if the Eddy current is absent.

Though the proposed EM drive is of switch type due to the requirement of disc oscillation for a gyroscope, the entire device can be regarded as an electrical motor as long as the

drive logic circuit is changed to be "successive" in the same direction of disc rotation, instead of "switched" in direction. That is, micro-scale electric motors can be implemented by the proposed design.

The 3-phase AC drive circuit design and the experimental simulation for the proposed EM drive module have been undertaken by our laboratory and will be reported shortly.

REFERENCES

[1] C. W. Lai, S. K. Hsiung, C. L. Yeh, A. Chiou, G. B. Lee, "A cell delivery and pre-positioning system utilizing microfluidic devices for dual-beam optical trap-and-stretch," *Sensors and Actuators B: Chemical*, vol. 135, pp. 388-397, 2008.
[2] J. Cho, T. Wiser, C. Richards, D. Bahr, R. Richards, "Fabrication and characterization of a thermal switch," *Sensors and Actuators A: Physical*, vol. 133, pp. 55-63, 2007.
[3] C. Acar, "Robust Micromachined Vibratory Gyroscope," Ph.D. Thesis, Universuty of California at Berkeley, 2004.
[4] N.-C. Tsai, C.-Y. Sue, "Fabrication and Analysis of a Micro-machined Tri-axis Gyroscope," *Journal of Micromechanics and Microengineering*, vol. 18, p. 115014, 2008.
[5] R. linnemann, P. Woias, C. D. Senfft, J. A. Ditterich, "A Self-Priming and Bubble-Tolerant Piezoelectric Silicon Micropump for Liquids and Gases", Proceedings IEEE Micro Electro Mechanical Systems, 1998, pp. 532-537.
[6] L. S. Fan, Y. C. Tai, R. S. Muller, "IC-Processed Electrostatic Micro-motors," Tech Dig Int Electron Devices Meeting, 1988. IEDM '88. Technical Digest., 1988, pp. 666-669.
[7] A. Beyzavi, N. T. Nguyen, "Modeling and optimization of planar microcoils", *Journal of Micromechanics and Microengineering*, vol. 18, p. 095018, 2008.
[8] C. H. Ahn, M. G. Allen, "A Comparison of Two Micromachined Inductors (Bar- and Meander- Type) for Fully Integrated Boost DC-DC Power Converters", *IEEE Transactions on Power Electronics*, vol. 11, pp. 239-245, 1996.
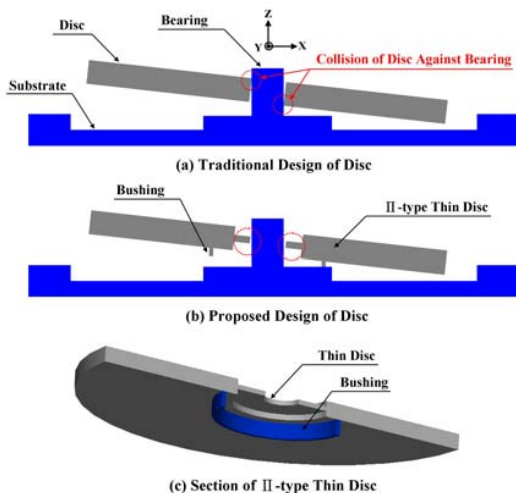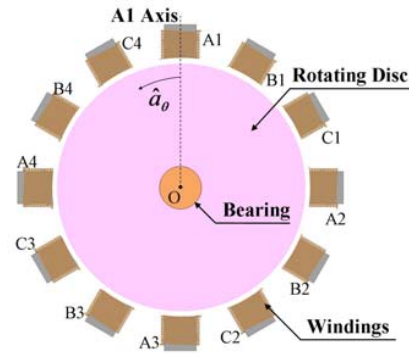
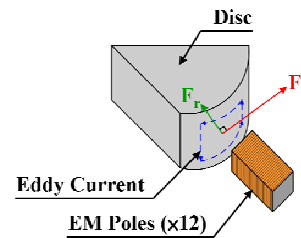Fig. 2 Allocation of the EM Poles Enclosing the Disc

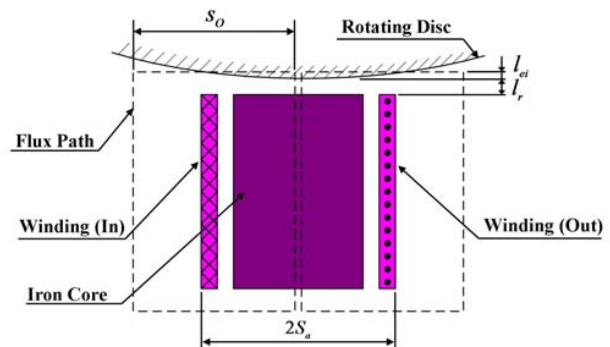

Fig. 3 Tangential and Radial Magnetic Forces Induced by EM Poles

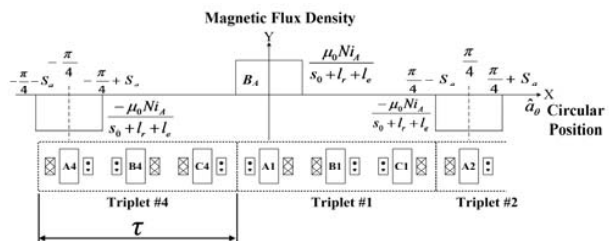Fig. 4 The Path of Magnetic Flux Circling the EM Pole

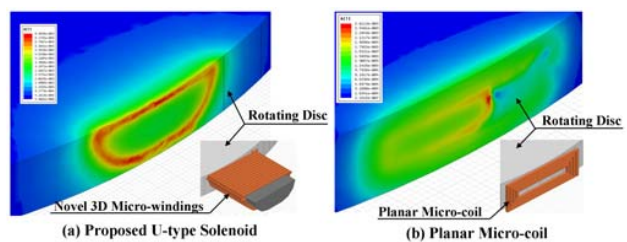Fig. 5 Magnetic Flux Density along the Circular Position of Disc

Fig. 1 Tilt of Rotating Disc Used for Gyroscopes

Fig. 6 Induced Magnetic Flux Distribution Along the Disc Brim
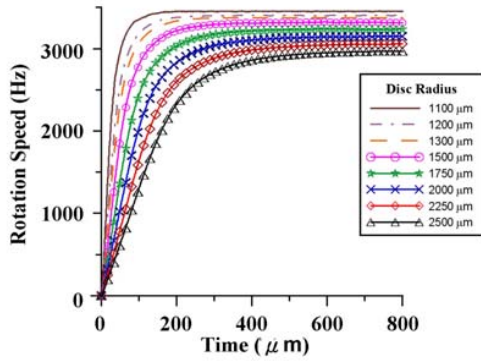
Fig. 7 Step Response of the Disc under Various Disc Radius

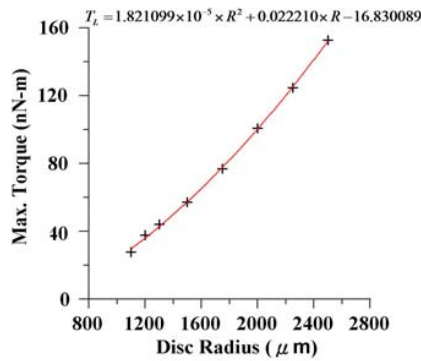$$T_L = 1.821099 \times 10^{-5} \times R^2 + 0.022210 \times R - 16.830089$$

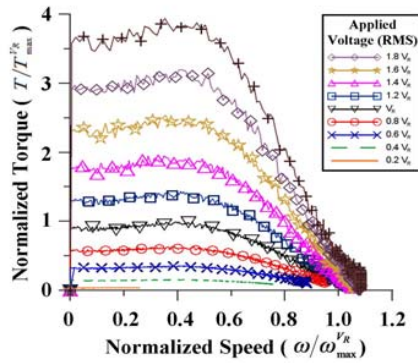Fig. 8 Torque of Disc Versus Disc Radius

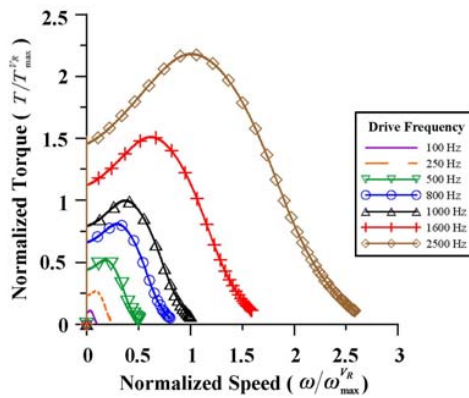Fig. 9 Torque / Speed Curve under Various Applied Voltage

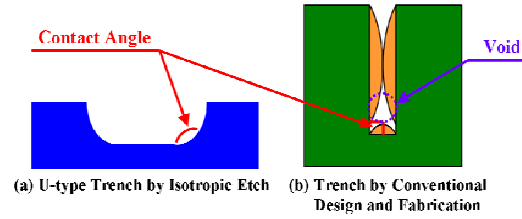Fig. 10 Torque Versus Speed under Various Drive Frequencies

Fig. 11 Comparison between Conventional Trench and U-type Trench
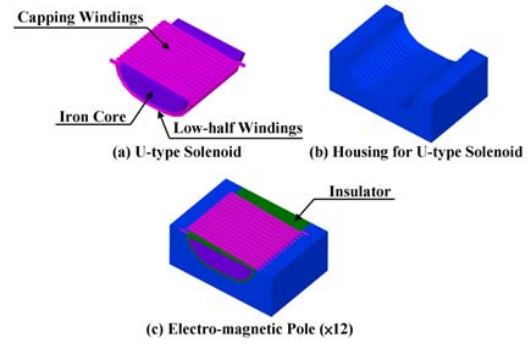(Proposed by this paper)

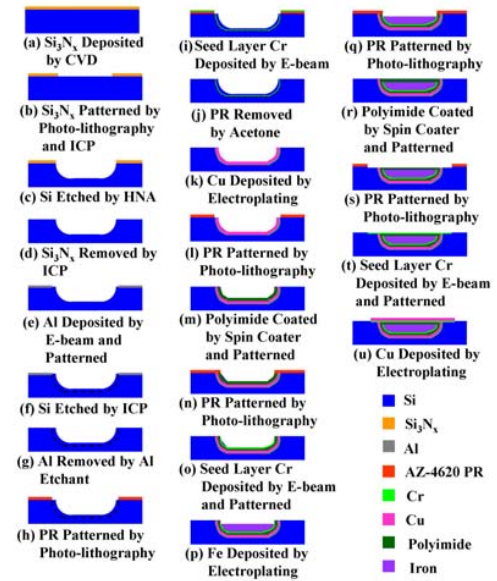Fig. 12 Innovative Design of Electromagnetic Poles
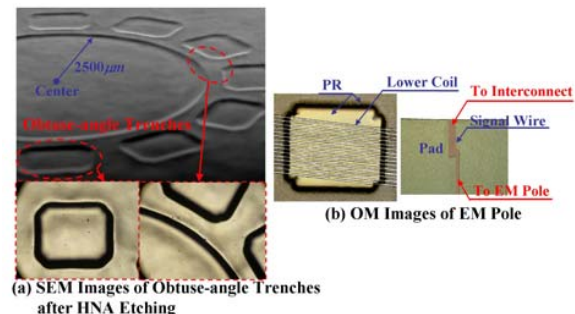

Fig. 13 Fabrication Process of U-type Electromagnetic Poles

Fig. 14 SEM and OM Images of U-type EM